Thermochimica Acta, 20 (1977) 115–139
© Elsevier Scientific Publishing Company, Amsterdam – Printed in The Netherlands

A HIGH SENSITIVITY DC THERMOMETRIC CIRCUIT USING OPERATIONAL AMPLIFIERS AND A HYBRID COMBINATION OF NTC AND PTC THERMISTORS

ALAN E. VAN TIL* AND DENNIS C. JOHNSON
Department of Chemistry, Iowa State University Ames, Iowa 50011 (U.S.A.)

ABSTRACT

Equations predicting the response of thermometric circuits constructed from operational amplifiers with NTC and NTC–PTC hybrid thermistors are derived and tested. Sensitivities and time constants were determined experimentally and are compared with theoretical predictions. The circuit with the NTC–PTC hybrid is characterized by greater sensitivity than a NTC circuit and greater linearity than a PTC circuit.

INTRODUCTION

The theoretical sensitivity of 6.6×10^{-9}°C nA^{-1} for a proposed temperature sensor utilizing a MOS transistor with pyroelectric material on the gate has not yet been achieved[1]. Existing circuits are continually being revised to increase sensitivity and linearity of response. Linde et al.[2] initiated modern thermometric titrimetry in 1953 by employing a thermistor with a negative temperature coefficient (NTC) as one arm of a dc Wheatstone bridge. Since that time, increased thermistor bridge sensitivity has been achieved in various ways including use of two or more NTC thermistors in parallel as one arm of the bridge[3–5]. Electronic amplification has been reported for dc[6, 7] and ac bridges[8, 9]. The ac bridges use sine-wave voltages although square-wave voltage has been proposed[10]. Detection limits of 5–10 μ°C have been reported for several instruments[9].

A non-linear response is observed in the bridge offset potential because of the parallel arrangement of bridge resistances and the nature of the semiconductor material in the thermistor. Numerical methods have been applied for linearization of bridge output[11, 12]; their use is tedious and requires electronic computational facilities. Analog linearization has been achieved by the use of resistors for thermistor-shunting networks with some sacrifice of sensitivity[13, 14].

Steady-state response of thermistors has been adequately treated by Buhl[15].

* Present address, Corporate Research, UOP Inc., Des Plaines, Ill. 60016, U.S.A. Author to whom correspondence should be sent.

Transient thermistor response including response times and problems of undershoot and overshoot are generally ignored in analytical applications. Hence, application is limited to slow reactions or when transient response is to be ignored. We have found that critical damping of the measurement system is easily achieved when those circuit and experimental parameters affecting transient response are identified and properly adjusted.

The construction and operation of dc thermistor circuits are simple. We have modified the basic circuit of Vanderborgh and Spall[16] in an effort to achieve theoretical output and an improvement in linearity of temperature response. A schematic of the circuit is shown in Fig. 1. Improvements achieved include elimination of loading of the bridge power supply by use of operational amplifiers as ideal current sources and incorporation of NTC thermistors with positive temperature coefficient (PTC) thermistors for an increase of bridge sensitivity by a factor of 5 × over the straight NTC circuits. This NTC–PTC hybrid circuit is intended primarily for single cell calorimetry. We describe here the steady-state behavior of the thermistor network,

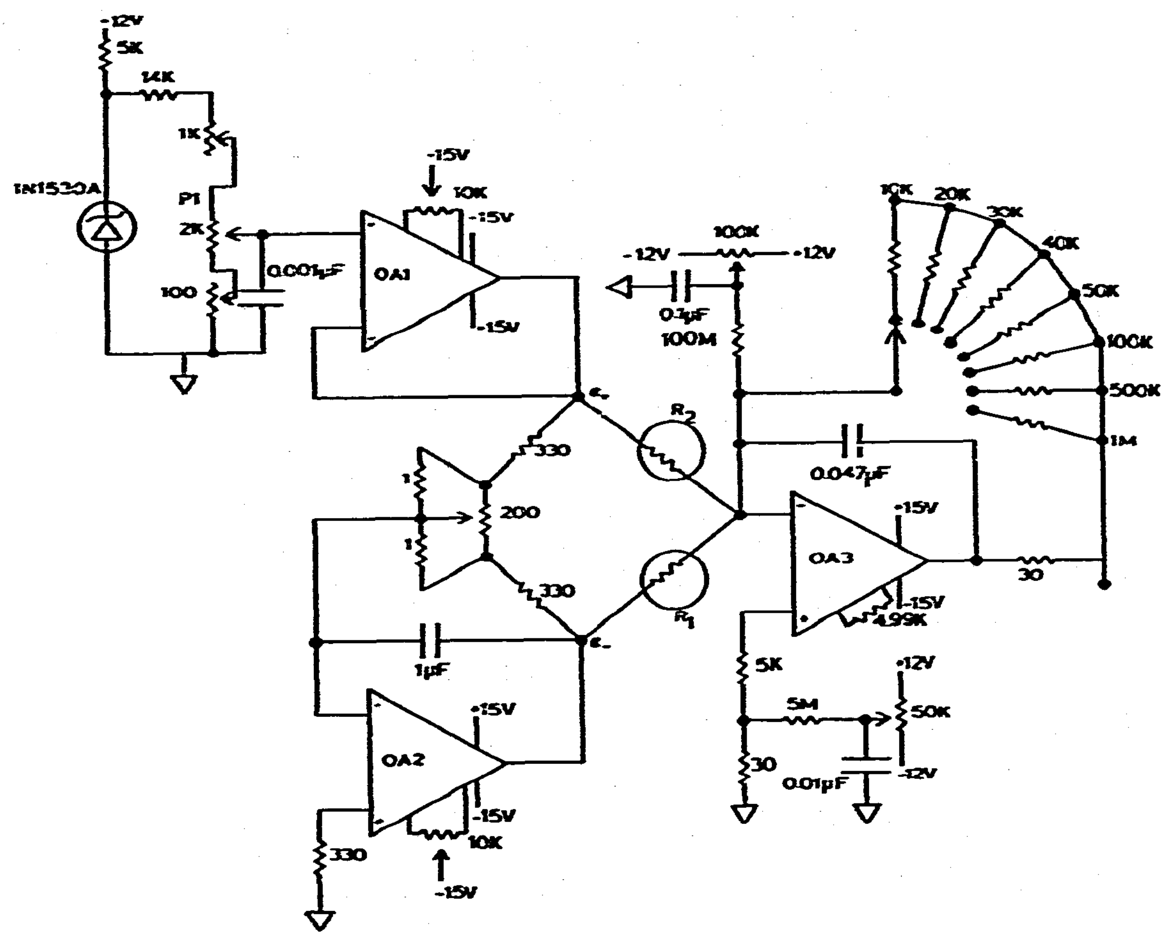

Fig. 1. Circuit diagram of thermistor bridge.

the effect of the thermistor dissipation constant on transient response, and the effect of various solution parameters on the temperature sensitivity and response time.

THEORETICAL

Circuit response to thermistor temperature change

The semi-conductor equation for a NTC thermistor is given by eqn (1)[13,17,18]. Definitions of regularly used symbols are

$$R_t = Z_t \exp\{\beta_t/T_t\} \tag{1}$$

given in Appendix A. Equation (1) is frequently written in the form

$$\ln R_t = z_t + \beta_t/T_t \tag{2}$$

where $z_t = \ln Z_t$. Equation (2) can be differentiated with respect to T_t to yield

$$\frac{1}{R_t}\frac{dR_t}{dT_t} = -\frac{\beta_t}{T_t^2} + \frac{1}{T_t}\frac{d\beta_t}{dT_t} + \frac{1}{Z_t}\frac{dZ_t}{dT_t} \tag{3}$$

The quantity $(1/R_t)(dR_t/dT_t)$ is called the temperature coefficient of resistance of the thermistor. The value of $(1/T_t)(d\beta_t/dT_t) + (1/Z_t)(dZ_t/dT_t) \ll -\beta_t/T_t^2$ and is frequently ignored. Thus,

$$\frac{1}{R_t}\frac{dR_t}{dT_t} \simeq -\frac{\beta_t}{T_t^2} \tag{4}$$

Equation (1) is known as the zero power equation and applies only in the case when negligible electrical power is dissipated by the thermistor. Buhl[15] has considered steady-state thermistor response in the case of appreciable power dissipation.

The output potential of operational amplifier OA-3 in Fig. 1 is related to the resistance of thermistors in positions t_1 and t_2 (R_1 and R_2) by eqn (5). Under conditions of negligible power dissipation, Equations (1) and (5) are

$$e_{o,3} = -\left(\frac{R_f}{R_1}\right)e_- - \left(\frac{R_f}{R_2}\right)e_+ \tag{5}$$

combined and differentiated to yield the temperature response of the circuit. For NTC thermistors, $d\beta/dT$ is positive and

$$\frac{de_{o,3}}{dT} = -\frac{R_f e_-}{R_1}\left(\frac{\beta_1}{T_1^2} - \frac{1}{T_1}\frac{d\beta_1}{dT_1} - \frac{1}{Z_1}\frac{dZ_1}{dT_1}\right) - \frac{R_f e_+}{R_2}\left(\frac{\beta_2}{T_2^2} - \frac{1}{T_2}\frac{d\beta_2}{dT_2} - \frac{1}{Z_2}\frac{dZ_2}{dT_2}\right) \tag{6}$$

the term $(1/T)(d\beta/dT)$ tends to decrease the sensitivity of $e_{o,3}$ with increased temperature. However, dR_t/dT_t is negative and the sign of $de_{o,3}/dT$ is positive.

For $T_1 = T_2 = T$ and $e_+ = -e_- = E$, the equation resulting when $\beta_1 \neq \beta_2$ may be written

$$\frac{de_{o,3}}{dT} = \frac{R_f E}{T^2}\left[\frac{\beta_1}{R_1} - \frac{\beta_2}{R_2}\right] + \frac{R_f E}{T}\left[\frac{1}{R_2}\frac{d\beta_2}{dT} - \frac{1}{R_1}\frac{d\beta_1}{dT}\right]$$

$$+ R_f E\left[\frac{1}{R_2 Z_2}\frac{dZ_2}{dT} - \frac{1}{R_1 Z_1}\frac{dZ_1}{dT}\right] \quad (7)$$

Equation (7) is of the form of a quadratic equation which describes a parabola.

The properties and applications of PTC thermistors were reviewed by Andrich[19]. Methods of manufacturing PTC thermistors were described by Sauer and Fisher[20]. A plot of ln R_t for a PTC thermistor vs. T_t closely resembles the sigmoidal curves familar for potentiometric titrations. Over a restricted temperature interval (~5°C), the slope of the plot is large and the zero-power resistance is given by eqn (8)[21].

$$R_t = Z_t \exp\{\alpha_t T_t\} \quad (8)$$

Differentiation of Equation 8 yields

$$\frac{1}{R_t}\frac{dR_t}{dT_t} = \alpha_t + T_t\frac{d\alpha_t}{dT_t} + \frac{1}{Z_t}\frac{dZ_t}{dT_t} \quad (9)$$

The value of $\alpha_t \gg T_t(d\alpha_t/dT_t) + (1/Z_t)(dZ_t/dT_t)$. Thus,

$$\frac{1}{R_t}\frac{dR_t}{dT_t} \simeq \alpha_t \quad (10)$$

The value of the material coefficient for a PTC thermistor, α_t, can be more than 10 × that for a NTC thermistor, β_t. The sensitivity of temperature sensing circuits made with PTC thermistors is, therefore, greater than that for NTC circuits; so also is the non-linearity.

The combination of a NTC and a PTC thermistor in the circuit of Fig. 1 can result in a highly sensitive device for single cell thermometry which can be linearized by adjustment of e_- relative to e_+. Combining eqns (4), (5), and (10) and differentiating

$$\frac{de_{o,3}}{dT_t} = -\frac{R_f e_-}{R_{NTC}}\left(\frac{\beta_t}{T^2}\right) + \frac{R_f e_+ \alpha_t}{R_{PTC}} \quad (11)$$

Repeating the differentiation and setting the result equal to zero specifies the equality required for linear response.

$$\frac{R_f e_-}{R_{NTC}}\left(\frac{2\beta_t}{T_t^3} - \frac{\beta_t^2}{T_t^4}\right) = \frac{R_f e_+ \alpha_t}{R_{PTC}}^2 \quad (12)$$

For typical operating parameters ($\beta \simeq 4000$ and $T \simeq 300$°K)

$$\frac{\beta_t^2}{T_t^4} \gg \frac{2\beta_t}{T_t^3}$$

and linearity is achieved if

$$-\frac{e_-}{e_+} = \frac{\dfrac{\alpha_t^2}{R_{PTC}}}{\dfrac{\beta^2}{R_{NTC}T^4}} = \frac{\dfrac{1}{R_{PTC}^3}\left(\dfrac{dR_{PTC}}{dT}\right)^2}{\dfrac{1}{R_{NTC}^3}\left(\dfrac{dR_{NTC}}{dT}\right)^2} \tag{13}$$

Typically, linearity results if $-(e_-/e_+) \simeq 16$. Linearity may also be achieved with use of series NTC thermistors with the PTC thermistor such that

$$\sum_{i=1}^{n} \beta_i = \alpha_t.$$

Such a circuit also has greater sensitivity than the single NTC thermistor with the PTC thermistor.

Transient response

For small changes of temperature of an NTC thermistor through which $d\beta_t/dT_t$ can be ignored, the zero power operation (eqn (1)) can be described by eqn (14)

$$R_b = R_t \exp\left\{\beta_t\left[\frac{T_t - T_b}{T_t^2}\right]\right\} \tag{14}$$

where R_b is the value of R_t when $T_t = T_b$. Equation (14) is valuable for beginning a consideration of the response of R_t when the bulk media surrounding the thermistor is heated at a rate, γ_b, and $T_t \neq T_b$. For small γ_b, $(T_b - T_t)/T_t^2 \simeq 0$ and the exponential term of eqn (14) can be accurately given by the first two members of an Euler series expansion. Thus,

$$R_b = R_t\left[1 + \beta_t\left(\frac{T_t - T_b}{T_t^2}\right)\right] \tag{15}$$

Rearranging eqn (15),

$$\Delta R_{b-t} = R_b - R_t = \frac{R_t\beta_t}{T_t^2}(T_t - T_b) \tag{16}$$

Combining eqns (4) and (16),

$$\Delta R_{b-t} = \frac{-dR_t}{dT_t}(T_t - T_b) \tag{17}$$

Carslaw and Jaeger[22] solved the problem of heat transfer between a sphere and the surrounding media. For the case of heat transfer from an electrically heated spherical thermistor to the surrounding media at zero initial temperature,

$$T'_t - T'_b = \frac{P_t}{8\pi r_t \lambda_t}\left\{1 + \frac{2\lambda_t}{h_t r_t} - \frac{12h_t}{\lambda_t}\sum_{n=1}^{\infty}\frac{\exp(-\alpha_n^2 D_t t)}{\alpha_n[r_t^2\alpha_n^2 + r_t h(r_t h - 1)]\sin r_t\alpha_n}\right\} \tag{18}$$

For the case of external heating of a spherical thermistor at zero initial temperature by the bulk media,

$$T''_t - T''_b = \frac{-\gamma_b r_t^2}{6D_t}\left\{1 + \frac{2\lambda_t}{h_t r_t} - \frac{12h_t}{\lambda_t}\sum_{n=1}^{\infty}\frac{\exp(-\alpha_n^2 D_t t)}{\alpha_n[r_t^2\alpha_n^2 + r_t h(r_t h - 1)]\sin r_t\alpha_n}\right\} \tag{19}$$

Our treatment of the heat transfer between a thermistor bead and the surrounding media assumes it to be a perfect sphere. The actual thermistor configuration used in this research resulted from mounting a thermistor bead with epoxy into the end of a Teflon cylinder having a diameter slightly greater than the diameter of the thermistor.

The time-independent portions of eqns (18) and (19) yield temperature differences across the thermistor bead material and thermal boundary layer when no extraneous material covers the thermistor. Correction factors must be applied to account for stem conduction and the surface film of epoxy. Initially, consider only the epoxy film. The second term of eqns (18) and (19) $(2\lambda_t/h_t r_t)$ is multiplied by a factor to yield the average temperature difference across the epoxy film plus the thermal boundary layer. From Fourier's law, dimensional analysis and geometrical considerations, the inner conductivity, λ_i, can be derived to replace λ_t in the second term by eqn (20).

$$\lambda_i = 2\lambda_t\left(\frac{r_t\lambda_e + x_e\lambda_t}{r_t\lambda_e}\right) \tag{20}$$

The equivalent conductivity, λ_{eq}, substituted for λ_t in the time-dependent terms of eqns (18) and (19) can be shown to be

$$\lambda_{eq} = 0.5\lambda_t\left(\frac{r_t\lambda_e}{r_t\lambda_e + x_e\lambda_t}\right) \tag{21}$$

The superposition principle commonly used for linear systems and in many problems of heat conduction is applied. Accordingly, the difference $T_t - T_b$ is assumed given by a linear combination of eqns (18) and (19). The prime and double prime designations in eqn (22) assist in recognizing

$$T_t - T_b = (T'_t + T''_t) - (T'_b + T''_b) \tag{22}$$

the equation ((18) or (19)) used to calculate the designated term.

So that the solution of eqn (17) is made more tractable, only the time-independent parts of eqns (18) and (19) are considered here. Simple calculations show that the second terms of eqns (18) and (19) control thermistor response. Hence, eqn (20) may be written as

$$T_t - T_b = \left(\frac{3P_t - 4\pi r_t^3 c_t \gamma_b}{12\pi r_t \lambda_t}\right)\left(\frac{\lambda_i}{h_t r_t}\right) \tag{23}$$

The time-independent parts of eqns (18) and (19) contain terms common to the thermistor dissipation constant, δ_t, and the thermistor time constant, τ_t.

$$\delta_t = \frac{\delta_o \delta_b}{\delta_o + \delta_b} = 8\pi r_t \lambda_t \left(\frac{h_t r_t}{h_t r_t + 2\lambda_i}\right) \tag{24}$$

$$\tau_t = \tau_o + \tau_b = \frac{r_t^2}{6D_t}\left(\frac{h_t r_t + 2\lambda_i}{h_t r_t}\right) \tag{25}$$

For rates of bulk fluid stirring which approach zero, $h_t r_t \rightarrow \lambda_b$,

$$\delta_t \rightarrow 8\pi r_t \lambda_t \left(\frac{\lambda_b}{\lambda_b + 2\lambda_i}\right) \tag{26}$$

$$\tau_t \rightarrow \frac{r_t^2}{6D_t}\left(\frac{\lambda_b + 2\lambda_i}{\lambda_b}\right) \tag{27}$$

For high rates of stirring, $h_t r_t \gg 2\lambda_i$, and

$$\delta_t \rightarrow 8\pi r_t \lambda_t \tag{28}$$

$$\tau_t \rightarrow \frac{r_t^2}{6D_t} \tag{29}$$

The non-linear dependence of δ_t on h_t as given by eqn (24) was demonstrated by Rasmussen[23].

Substitution of the time-independent parts of eqns (18) and (19) into eqn (22) and combining the result with eqn (17) yields

$$\frac{\Delta R_{t-b}}{dR_t/dT_i} = \frac{P_t}{8\pi r_t \lambda_t}\left(1 + \frac{2\lambda_i}{h_t r_t}\right) - \frac{\gamma_b r_t^2}{6D_t}\left(1 + \frac{2\lambda_i}{h_t r_t}\right) \tag{30}$$

Since $D_t = \lambda_t / c_t$,

$$\frac{-dR_t}{dT_t} = \frac{\lambda_t \Delta R_{b-t}}{\left[\frac{P_t}{8\pi r_t}\left(1 + \frac{2\lambda_i}{h_t r_t}\right) - \frac{\gamma_b r_t^2 c_t}{6}\left(1 + \frac{2\lambda_i}{h_t r_t}\right)\right]} \tag{31}$$

Hence, the temperature coefficient of resistance for the thermistor, $dR_t/R_t dT_t$, is directly related to its thermal conductivity, λ_t, as discussed by Kudryavtsev et al.[24].

Combining eqns (24), (25) and (30) yields

$$\tau_t = \left(\frac{P_t}{\delta_t} + \frac{\Delta R_{b-t}}{\mathrm{d}R_t/\mathrm{d}T_t}\right)\frac{1}{\gamma_b} \tag{32}$$

Using the definition $P_t = C_t\gamma_t$,

$$\tau_t = \frac{C_t\gamma_t}{\delta_t\gamma_b} + \frac{\Delta R_{b-t}}{\mathrm{d}R_t/\mathrm{d}T_t}\left(\frac{1}{\gamma_b}\right) \tag{33}$$

In the limit where $\gamma_b \rightarrow \infty$, eqn (33) becomes

$$\tau_t = \frac{C_t\gamma_t}{\delta_t\gamma_b} \tag{34}$$

If $\gamma_t = \gamma_b$,

$$\tau_t = \frac{C_t}{\delta_t} \tag{35}$$

This equality is experimentally valid only if the thermistor is suspended by its leads such that the thermistor surface is uniformly accessible.

Equation (32) can also be written

$$\tau_t = \frac{\Delta R_{b-t}}{\mathrm{d}R_t/\mathrm{d}T_t}\left(\frac{1}{\gamma_b - \gamma_t}\right) \tag{36}$$

Because $\mathrm{d}R_t/\mathrm{d}T_t$ is negative for a NTC thermistor, $\Delta R_{b-t}/(\gamma_b - \gamma_t)$ is negative. Increasing P_t will decrease the effect of γ_b on T_t and the slope of a plot of T_t vs. $1/\gamma_b$ will decrease.

The convective heat transfer coefficient, h_t, in eqn (31) is part of the Nusselt number, Nu,

$$Nu = \frac{h_t r_t}{\lambda_b} \tag{37}$$

For a stirred media, Nu is related to the Prandtl, Pr, and Reynolds, Re, numbers by equations of the general form

$$Nu = \mathrm{a}Re^{\mathrm{b}}Pr^{\mathrm{c}} \tag{38}$$

where a, b, and c are constants and Re and Pr are defined

$$Re = \frac{U}{\nu_b}$$

$$Pr = \frac{\nu_b}{D_b}$$

A sphere is a poorly streamlined body and separation of boundary layer flow occurs for $Re > 50$. For the stirred systems of interest in calorimetry ($10^3 < Re < 10^4$), the bulk fluid is fully turbulent and the hydrodynamic boundary layer around the thermistor is laminar with separation. Kutateladze[25] determined that for a sphere, the diameter Nusselt number is

$$Nu_d \simeq 2 + 0.35\, Re^{0.58} Pr^{0.36} \tag{39}$$

The radius Nusselt number is

$$Nu_r = 1.00 + 0.175\, Re^{0.58} Pr^{0.36} \tag{40}$$

Murdock et al.[26] showed that

$$h_t r_t = (N_s r_t)^{0.6} \tag{41}$$

where N_s is the rotation speed of the bulk media stirrer in units of rev min^{-1}. Rice et al.[27] determined that the fluid velocity, U, at a distance r from the axis of stirrer rotation and in the plane of the stirrer is given by

$$U(r) = \frac{2\pi r_s^2 N_s}{60r} \tag{42}$$

Equation (42) is valid for distances up to half way from the outer edge of the stirrer to the cell wall. Combining eqns (34)–(41)

$$\frac{h_t r_t}{\lambda_b} = 0.50 + 0.0875 \left(\frac{r_s^2 \omega_s 2r_t}{r v_b}\right)^{0.58} \left(\frac{v_b c_b}{\lambda_b}\right)^{0.36} \tag{43}$$

The coefficient of the second term in eqn (43) was calculated for direct exposure of one half the thermistor surface to the solution. When $\omega_s = 0$,

$$h_t r_t = 0.50\, \lambda_b$$

and from eqn (26),

$$\delta_t = 4\pi r_t \lambda_t \left(\frac{\lambda_b}{0.5\lambda_b + 2\lambda_i}\right) \tag{44}$$

Application of a thermistor to determine values of the thermal conductivity of the bulk fluid was performed by Papadopoulos[28].

The Pai power series for calculating the velocity distribution in a pipe can also be applied to calculation of Re for use in eqn (40)[29].

$$\frac{U(r)}{U_{max}} = 1 + a_1 \left(\frac{r}{r_c}\right)^2 + a_2 \left(\frac{r}{r_c}\right)^{2m} \tag{45}$$

In eqn (45):

$$U_{max} = \omega_s r_s$$

$$a_1 = \frac{n - m}{m - 1}$$

$$a_2 = \frac{1-n}{m-1}$$

$$m = -0.617 + 8.21 \times 10^{-3}\,(Re_{\max})^{0.786}$$

$$n = 0.585 + 3.17 \times 10^{-3}\,(Re_{\max})^{0.833}$$

and

$$Re_{\max} = \frac{\omega_s r_s 2r_c}{\nu_b}$$

The values of $U(r)/U_{\max}$ calculated from eqns (42) and (45) are different. The lack of agreement occurs because of the calculation of the cell velocity profile in the plane of the stirrer (eqn (45)) vs. that outside the plane of the stirrer (eqn (42)). Equation (46) should be used when the thermistor is in the plane of the stirrer.

$$Re_t = \frac{U(r) r_s \omega_s 2r_t}{U_{\max} \nu_b} \tag{46}$$

Rewriting eqn (16) as

$$\frac{\Delta R_{b-t}}{R_t(T_t - T_b)} = \frac{\beta_t}{T_t^2} \tag{47}$$

and substituting into eqn (6) yields

$$\frac{de_{o,3}}{dT} = -\left[\frac{R_f e_-}{R_1^2}\,\frac{\Delta R_{b-t,1}}{(T_1 - T_b)}\right] - \frac{R_f e_+}{R_2^2}\left[\frac{\Delta R_{b-t,2}}{(T_2 - T_b)}\right] \tag{48}$$

Combining eqns (23) and (48) and writing only half of the equation corresponding to R_1

$$\frac{de_{o,3}}{dT} = -\frac{R_f e_-}{R_1^2}\left[\frac{12\pi r_{t,1}\lambda_t \Delta R_{b-t,1}}{(3P_{t,1} - 4\pi r_{t,1}^3 c_t \gamma_b)}\left(\frac{h_{t,1} r_{t,1}}{\lambda_{t,1}}\right)\right] + \ldots \tag{49}$$

Combining eqns (43) and (49)

$$\frac{de_o}{dT} = -\frac{R_f e_-}{R_1^2}\cdot$$

$$\left\{\frac{r_{t,1}\lambda_t \Delta R_{b-t,1}(18.8\lambda_{b,1} + 3.30\lambda_{b,1})\left(\frac{r_{s,1}^2 \omega_{s,1} 2r_{t,1}}{r_1 \nu_b}\right)^{0.58}\left(\frac{\nu_b c_b}{\lambda_b}\right)^{0.36}}{\lambda_{t,1}(3P_{t,1} - 4\pi r_{t,1}^3 c_t \gamma_b)}\right\} \tag{50}$$

Examination of eqn (50) reveals that de_o/dT gains decreased dependency on γ_b as P_t increases. This fact is important in thermokinetic studies since uniform response to change of solution temperature is needed when the rate of the chemical reaction is time dependent.

When $\gamma_b = 0$ and $\omega_s = 0$, eqn (50) reduces to

$$\frac{de_o}{dT} = -\frac{R_f e_-}{R_1^2}\left[\frac{6.28 r_{t,1}\lambda_t \Delta R_{b-t,1}\lambda_{b,1}}{\lambda_{i,1}P_{t,1}}\right] + \ldots \tag{51}$$

Implicit in the derivation of eqn (39) was the assumption that thermal conduction of the thermistor support is negligible. Dutt and Stickney[30] demonstrated that conduction errors are only negligible if the thermal sensor is mounted on a support of low thermal conductivity. Contact resistance between the thermistor and mount is also important. Since no perfect insulator exists, a stem correction was applied to eqn (20). Without stem correction, the tip solution predicts excessive tip temperature and time constants[31].

For the thermistor probe design used in this research, correction was made only for the exposed portion of Teflon tubing in which the head was mounted. Correction applied to eqn (20) yields

$$\lambda_i = \frac{2\lambda_t^2}{\lambda_c}\left(\frac{h_s r_{st}}{\lambda_s}\right)\left(\frac{r_t\lambda_c + x_c\lambda_t}{r_t\lambda_s + x_s\lambda_t}\right) \tag{52}$$

in which λ_s is calculated from

$$\lambda_s = \frac{\lambda_c A_c + \lambda_w A_w}{A_t}$$

and h_s from

$$Nu_d = 0.478\, Re^{0.5} Pr^{0.3}$$

as described by Scadron and Warshawsky[32] for cylinders in a crossflow.

An area correction must also be applied to the time-dependent portions of eqn (19). The exponential term is multiplied by the reciprocal of the fractional area of the thermistor exposed to the solution (2 for our case). The equivalent conductivity, λ_{eq}, corrected for stem conduction is given by

$$\lambda_{eq} = 0.5\left[\lambda_t\left(\frac{r_t\lambda_c}{r_t\lambda_c + x_c\lambda_t}\right) + \lambda_t\left(\frac{r_t r_s h_s}{r_t\lambda_s + x_s\lambda_t}\right)\right] \tag{53}$$

EXPERIMENTAL

Instrumentation and apparatus

The NTC bead thermistor probes were Type 44031 from Yellow Springs Instrument Co. They were chosen because of low manufacturing tolerances (10,000 Ω ± 0.5%) and excellent long term stability. The PTC thermistors were Positemp Type 713T15 from Pennsylvania Electronics Technology, Inc., and were nominally 10,000 Ω at 25°C. The thermistors were mounted as shown in Fig. 2. A common junction box mounted on the calorimeter head was used for all connections between the amplifier circuit and thermistor leads.

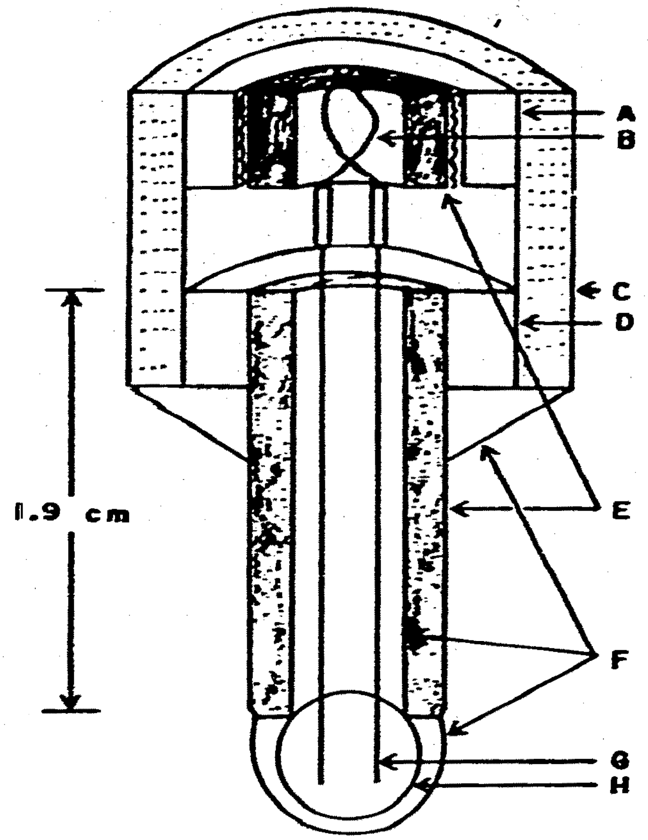

Fig. 2. Cross-section of thermistor probe. A = Tygon tubing; B = thermistor lead wires (copper); C = Pyrex tube (probe); D = Tygon tubing; E = Teflon tubing; F = epoxy; G = thermistor lead wires (platinum); and H = thermistor bead.

The amplifier circuit is shown schematically in Fig. 1. Thirty-inch coaxial cable was used for connection of the circuit with thermistor probes. A conventional 110 V ac regulator from Applied Research Laboratories was used in series with a Wanlass Model CVR-120 regulator for line voltage regulation. After six months of successful operation of the circuit in Fig. 1, the long term stability was improved by substituting Analog Devices 504J amplifiers for AO1 and OA2. The circuit was also constructed on a printed circuit board to decrease stray capacitances found for point-to-point wiring. This modification is referred to as Circuit B.

Procedures

Calibration of the bridge and amplifiers was made by substituting decade resistance boxes adjustable to $\pm$ 1 Ω for the thermistors. Circuit parameters were $R_f = 1.0016 \times 10^6\ \Omega$ and $e_+ = -e_- = 0.50000$ V to insure high sensitivity and a zero power approximation. The decade resistance boxes were calibrated by Physics Instrument Services of Iowa State University. Thermistor resistances were measured at approximately three-degree intervals in the range 0–48 °C. Solution temperatures were read from a partial immersion Hg thermometer to $\pm$ 0.01 °C. The Hg thermometer was calibrated at four points maintaining a stem temperature of 25.0 $\pm$ 0.5 °C. The four points were: the ice point, 0.000 °C; the $NaCl$–Na_2SO_4–H_2O eutectic, 17.878 °C[12]; the Na_2SO_4–H_2O eutectic, 32.383 °C[12]; and the freezing point of sublimed phenol, 40.85 °C[33]. The last reference point was given the least significance because of the difficulty of obtaining phenol which is free of cresols. Solution temperatures were measured by the Hg thermometer at a point 1 in. from the thermistor bead.

The temperature control bath used in thermistor resistance measurements was a 10-l plastic tub filled with water and resting on a magnetic stirrer. Temperature control for the bath involved circulation of water at 1 l min^{-1} from a 20-l Sargent thermostated bath controlled to $\pm$ 0.01 °C through an immersed 50-ft. coil of 0.5 in. polystyrene tubing.

The isoperibol differential calorimeter used for measurement of circuit sensitivity ($e_{o,3}$ vs. T) consisted of two glass Dewars, matched in size and thermal characteristics, with stirrers and electrical resistance heaters. The stirrers were perforated Teflon disks with 1.27-cm radius and 3.18-mm thickness operating at 800 rev min^{-1}. The heaters were 30-Ω metal-film resistors coated with epoxy resin. This calorimeter was also used for thermometric titrations and a complete description will be given in a subsequent publication.

The temperature sensitivity of the thermometric circuit was measured using only one calorimeter cell after replacing one thermistor in the bridge by a 10,088 $\pm$ 1 Ω metal-film resistor. This resistor was mounted on a heat sink in the junction box. A 250-ml volume of deionized water in the cell was electrically heated and T_b and the corresponding value of $e_{o,3}$ measured. All potentials were measured with a Corning Digital 112 pH meter in the mV mode or a Leeds and Northrup K-2 potentiometer readable to $\pm$ 5 μV. The Corning meter was calibrated with the K-2 potentiometer against an unsaturated Weston cell with a potential of 1.01891 absolute volts at 25.0 °C. The Weston cell was calibrated 2 October 1973 by Ames Laboratory USAEC at Ames, Iowa, against four parallel Weston cells standardized periodically against a cell from the National Bureau of Standards.

Solution temperatures for determination of circuit sensitivity were measured with a Parr 1622 bomb calorimeter thermometer (5E2808) which was calibrated 23 May 1973 by Parr Instrument Co. against a National Bureau of Standards platinum resistance thermometer. The calibration was made with full immersion and stem corrections for partial immersion in our experiments were made according to the procedure of Swindells[34].

Thermistor response to a step change in temperature and the thermal time constant were determined by two methods. Method 1: The thermistor was heated electrically after the manner of Papadopoulos[28] and the return to equilibrium temperature followed. Method 2: The thermistor probe was plunged into a solution at a temperature other than ambient according to the method of Pharo[25]. Bridge output was monitored by a Heath EU-20W recorder without damping.

Measurement of time constant vs. heating rate was made with unperforated disk stirrers of different radii at velocities of 45.0–207.3 rad sec^{-1}. Rotational velocities were determined by a Sanborn 7701 oscillograph. Controlled heating rates were provided by a Sargent Coulometric Current Source connected to the resistance heater in the cell.

Circuit noise and drift were measured after substitution of 10 kΩ metal-film resistors for the two thermistors. Other circuit parameters were $e_+ = -e_- = 1.00000$ V, $R_f = 1.0016 \times 10^6$ Ω and $C_f = 0.047$ μF. $e_{o,3}$ vs. time was recorded for 33 hr on the Heath recorder at a sensitivity of 1.130 mV $in.^{-1}$. The recovery time of the circuit to application of a 100 mV step function to the output of OA1 was measured with a Hewlett-Packard 122A oscilloscope.

Further experimental details may be found in ref. 36.

RESULTS AND DISCUSSION

Power supply stability

The power supply described had required little adjustment over a one-year period of successful operation. Typical stability was determined by measurement of e_+, e_- and $|e_+ - e_-|$ at irregular intervals over a two-week period with at least one measurement per working day. The results fitted by a linear least squares method are:

$$e_+ = 1000.0 \pm 0.02 \text{ mV} - 0.0025 \pm 0.0021 \text{ mV/day}$$

$$-e_- = 1000.2 \pm 0.02 \text{ mV} - 0.001 \pm 0.0021 \text{ mV/day}$$

$$|e_+ - e_-| = 0.175 \pm 0.007 \text{ mV} + 0.003 \pm 0.001 \text{ mV/day}$$

With the bridge connected and 10 kΩ metal-film resistors replacing the thermistors, the peak-to-peak noise and drift over a 24-h period was 10 ppm for a room temperature constant to $\pm$ 1 °C. Recovery time from a transient voltage applied to the output of OA1 was 0.3 sec for $C_f = 0.047$ μF. Circuit B had a peak-to-peak noise of 7 ppm for $C_f = 2$ μF. Distinct advantages of this circuit are the absence of loading of the power supply and easy adjustment of the sensitivity of the thermistor bridge by the adjustment of potentiometer P1 (see Fig. 1).

Thermistor material parameters

The value of β_t for thermistor t_1 and t_2 (both NTC) were determined at the standard temperature reference points cited earlier. Plots of β_t vs. T_t were nearly linear and were analyzed by a linear least squares computer program. The results are:

$$\beta_1 = 3.3816 \pm 0.0373 \text{ T (K)} + (2.5506 \pm 0.0111) \times 10^3 \text{ K}$$

$$\beta_2 = 3.3378 \pm 0.0426 \text{ T(K)} + (2.5634 \pm 0.0127) \times 10^3 \text{ K}$$

The uncertainties given are deviations for 95% confidence. At 25.00 °C,

$$\beta_1 = 3558.8 \pm 1.5 \text{ K}$$

$$\beta_2 = 3558.5 \pm 1.7 \text{ K}$$

Thermistor resistance data was obtained in the temperature range 24.929–25.080 °C and dR_t/dT_t calculated by eqn (1). Results are given in Table 1. Values of Z_t and dZ_t/dT_t at 25.00 °C were approximated from resistance data obtained at

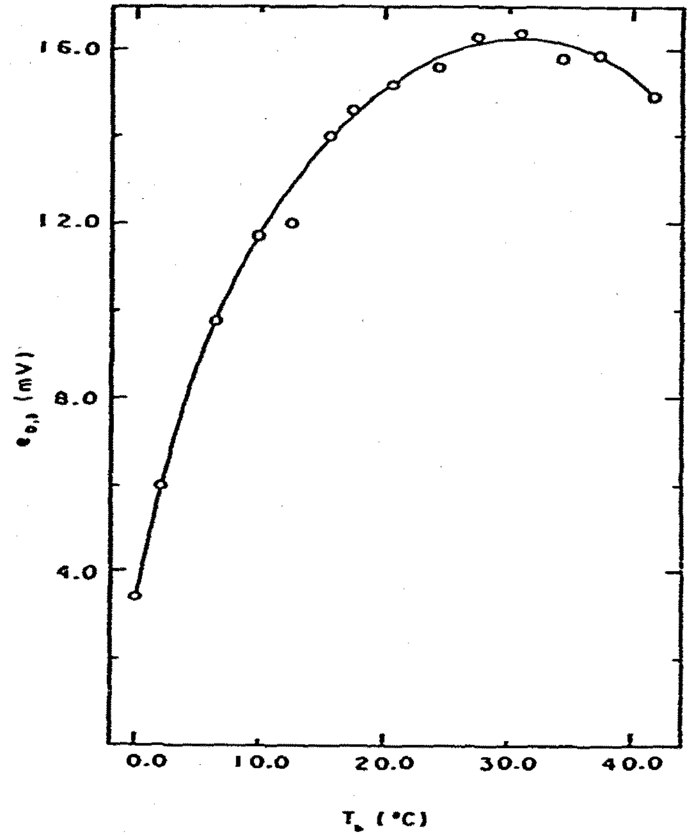

Fig. 3. Error curve for thermistor t_2 vs. t_1.

24.08 and 26.03°C. The results are included in Table 1. The approximate value of dR_t/dT_t from eqn (4) was used for the remaining work because all temperature intervals were 2°C or less.

A strong criticism of differential thermometric titrimetry is the impossibility to date of obtaining identical sensitivities for two thermistors. The origin of this problem can be seen by noting the differences in material parameters for even the closely matched thermistors in Table 1. An experimental error curve ($e_{o,3}$ vs. T_b) is shown in Fig. 3 for the two thermistors described in Table 1. The slope of the curve is very small except at temperatures considerably below 25°C and, presumably, greater than 45°C assuming the parabolic shape for the error curve predicted by eqn (7). Linear response can be obtained by adjustment of e_+ relative to e_-. Following the procedure similar to that for the NTC–PTC hybrid in eqns 11–13, it can be demonstrated that

$$-\frac{e_-}{e_+} = \frac{R_2\beta_2^2}{R_1\beta_1^2}$$

The calculated value of e_-/e_+ for linear response in this case is 1.00023 and the experimental value was determined to be 1.000185.

TABLE 1

THERMISTOR MATERIAL PARAMETERS AT 25 °C

Thermistor	R_t	$\mathrm{d}R_t/\mathrm{d}T_t$ *(eqn (3))*	$\mathrm{d}R_t/\mathrm{d}T_t$ *(eqn (4))*	Z_t	$\mathrm{d}Z_t/\mathrm{d}T_t$
$t_{NTC,1}$	$10{,}001 \pm 1\,\Omega$	$-3.9582 \times 10^{2}\,\Omega\,K^{-1}$	$-4.0035 \times 10^{2}\,\Omega\,K^{-1}$	$0.06545\,\Omega$	$-7.092 \times 10^{-4}\,\Omega\,K^{-1}$
$t_{NTC,2}$	$9{,}997 \pm 1\,\Omega$	$-3.9459 \times 10^{2}\,\Omega\,K^{-1}$	$-4.0031 \times 10^{2}\,\Omega\,K^{-1}$	$0.06565\,\Omega$	$-6.969 \times 10^{-4}\,\Omega\,K^{-1}$

TABLE 3

CUBIC EQUATION FOR TEMPERATURE RESPONSE

$e_{0,2}\,(\mathrm{mV}) = a + bT + cT^2 + dT^3$
$R_l = 100.04\,\mathrm{k}\Omega$; $N_s = 540$ rev min^{-1}; $C_t = 0.047\,\mu F$; $r_s = 1.27$ cm; 250.00 ml H_2O.

Thermistor	*E (V)*	*a(mV)*	*b(mV K⁻¹)*	*c(mV K⁻²)*	*d(mV K⁻³)*
$t_{NTC,2}$	0.50000	1.68507×10^{2}	-3.36247×10^{2}	1.807513×10^{1}	-1.95253×10^{-1}
t_{PTC}	0.50000	-1.03472×10^{5}	9.68844×10^{3}	-2.99636×10^{2}	3.18728
$t_{NTC,2} - t_{PTC}$	0.50000	-5.42410×10^{4}	3.46573×10^{3}	-4.65991×10^{1}	-1.29459×10^{-1}
$t_{NTC,2} - t_{PTC}$	1.00000	-7.92404×10^{4}	3.10707×10^{3}	6.76161×10^{1}	−2.47241
$(t_{NTC,1} + t_{NTC,2}) - t_{PTC}$	0.50000	-1.61952×10^{4}	1.46028×10^{3}	1.56476×10^{2}	−2.81641

Circuit sensitivity and noise

Attempts to increase temperature sensitivity of a thermistor bridge circuit have involved choice of thermistors with larger values of R_t because of the associated increase[37] in β_t. The signal-to-noise ratio suffers, however, because the thermistor noise is proportional to R_t^2. Sensitivity can be increased by use of larger bridge voltages as shown in eqn (7). For small temperature changes (< 1 °C) when $-e_- = e_+ = E$

$$\Delta e_{o,3}/\Delta T_b = -(R_f E/R_t)(\beta_t/T_t^2)$$

Experimental values of $\Delta e_{o,3}/\Delta T_t$ are given in Table 2 for a NTC thermistor. The results at $E = 0.5$ V agree with theory to 1 ppt. For bridge voltage > 0.5 V, self heating of the thermistor is significant and for our rate of stirring, $T_t \neq T_b$. Hence, R_t is less than in the absence of self heating and apparent sensitivity increases. The results in Table 2 at 1.0 V are in good agreement with theory when correction is made for self heating.

The temperature sensitivity for several thermistor configurations was determined over a 2-degree interval centered at 25 °C as shown in Fig. 4. The data was fitted to cubic equations for the purpose of comparing changes in linearity and sensitivity with temperature. The results are summarized in Table 3. For a small ΔT, the sensitivity is most easily approximated by the value of the coefficient b in Table 3. The sensitivity for a NTC–PTC hybrid is much greater than for a single NTC thermistor. A comparison of the sensitivity of our circuit with sensitivities for several dc circuits described in the literature is given in Table 4. The sensitivity of our circuit is the greatest of any reported to date and is in agreement with the theoretical prediction by eqn (7).

Uncertainty (noise) in the temperature measurement for various thermistors and thermistor combinations is given in Table 5. The value of ΔT_n was calculated from experimental data by the PARD convention[40] and represents the uncertainty in T_b for an isothermal solution as determined from the mean of $e_{o,3}$ over a 5-min recording period. It was interesting to note the successive decrease in ΔT_n as the

TABLE 2

SENSITIVITY DATA FOR $t_{NTC,1}$

$N_s = 540$ rev min^{-1}; $C_f = 0.047$ μF; 250 ml H_2O; $r_s = 1.27$ cm.

Run	*Points*	*E(V)*	R_t	ΔT_b (°C)	$\Delta e_{o,3}/\Delta T_b$ (mV °C^{-1})
1	11	0.50000	100.04 KΩ	0.497°C	200.3 ± 0.1
2	25	0.50000	100.04 KΩ	1.188°C	200.6 ± 0.1
3	20	1.00001	1.0016 MΩ	0.490°C	4,005 ± 2
4	40	1.00001	1.0016 MΩ	1.102°C	4,027 ± 1

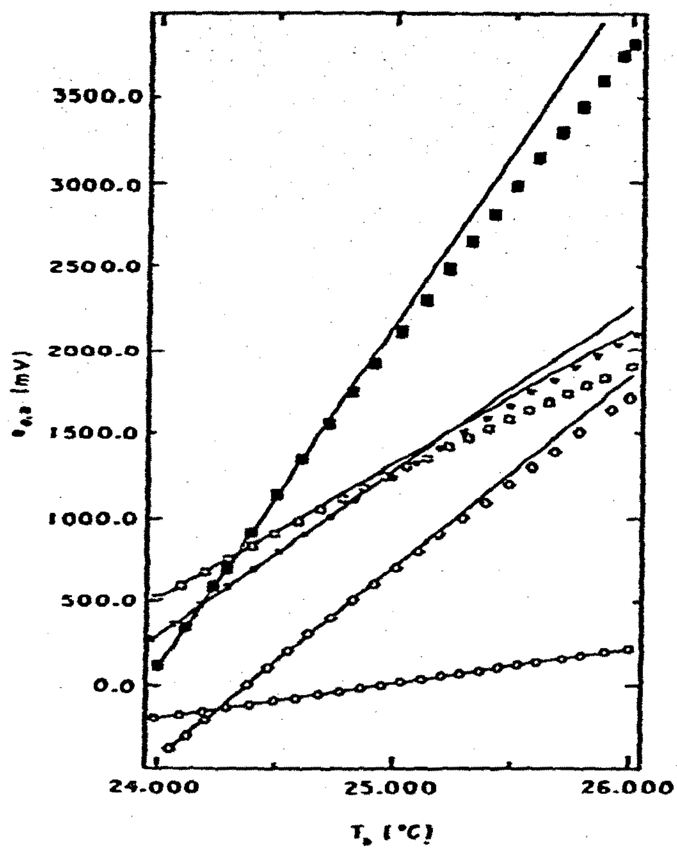

Fig. 4. Temperature sensitivity of thermistors. ○ = NTC, $e_+ = -e_- = 500.00$ mV; □ = PTC, $e_+ = -e_- = 500.00$ mV; ▽ = NTC–PTC, $e_+ = -e_- = 500.00$ mV; ■ = NTC–PTC, $e_+ = -e_- = 1000.00$ mV.

TABLE 4

COMPARISON OF SENSITIVITY FOR SEVERAL DC CIRCUITS

Reference	*Bridge voltage (V)*	*Thermistor resistance (kΩ)*	*Thermistor power (μW)*	*Circuit amplification*	*Sensitivity (mV °C⁻¹)*
38	12.000	100	not given	not given	139.5
5	2.037	5–5 in parallel	1037	100	3875
39	1.35	10	1.1	not given	417
this work (tsтc,1)	1.00000	10	100	100	4005

number of thermistors in the circuit is increased. Thermistors are generally accused of being noisy but we have found that the predominant sources of noise are stray electrostatic and electromagnetic pickup by the lead wires; the precaution of double shielding had a noticeable benefit to decrease ΔT_n. Maximum noise levels determined

TABLE 5

THERMISTOR CIRCUIT NOISE

Ref.	*Bridge voltage (V)*	*Amplifier damping*	ΔT_n (μ°C)
5	2.037	3 sec	50
37	12.000	not given	30

This work: $r_s = 1.27$ cm; $N_s = 540$ rev min^{-1}; $C_t = 0.047$ μF.

Thermistor	R_t		R_tC_t *(sec)*	*E (V)*	ΔT_n (μ°C)
$t_{STC,3}$	100.04	KΩ	0.005	0.50000	125
				1.00000	125
t_{PTC}	100.04	KΩ	0.005	0.50000	94
				1.00000	94
$t_{STC,3} - t_{PTC}$	100.04	KΩ	0.005	0.50000	50
				1.00000	60
$(t_{STC,1} + t_{STC,3}) - t_{PTC}$	100.04	KΩ	0.005	0.50000	43
$t_{STC,1}$	1.0016	MΩ	0.05	1.00000	25

TABLE 6

THERMISTOR DATA

Mn_3O_4:
$\rho_t = 4.21$ g cm^{-3} (ref. 41)
$\lambda_t = 1.76 \times 10^{-2}$ cal cm^{-1} sec^{-1} °C^{-1} (ref. 41)
$c_t' = 0.1547$ cal g^{-1}°C^{-1} (ref. 41)
$D_t = 2.70 \times 10^{-2}$ cm^2 sec^{-1} (calculated)

$BaTiO_3$ (1.5% Sr doped):
$\rho_t = 5.03$ g cm^{-3} (ref. 42)
$\lambda_t = 1.37 \times 10^{-2}$ cal cm^{-1} sec^{-1}°C^{-1} (ref. 42)
$c_t' = 0.105$ cal g^{-1}°C^{-1} (ref. 43)
$D_t = 2.59 \times 10^{-2}$ cm^2 sec^{-1} (calculated)

Epoxy resin:
$\lambda_e = 5.0 \times 10^{-4}$ cal cm^{-1} sec^{-1}°C^{-1} (ref. 44)

Dimensions:

	$t_{STC,1}$	$t_{STC,2}$	$t_{STC,3}$	t_{PTC}
r_t($\times 10^1$cm^{-1})	1.45	1.64	0.85	1.88
x_e($\times 10^2$cm^{-1})	6	6	6	12
x_s(cm)	0.7	0.7	1.2	1.2

by recording $e_{o,3}$ for a 1-h period are about 3 × the values in Table 5 which is in agreement with the observation of LaForce et al.[8].

Time constants

The calculations indicated by eqns (24), (25), (45) and (52) were programmed in WATFIV and executed on an IBM 360-5 digital computer at the Iowa State University Computation Center. A listing of the program is available on request from the authors. Although exact specifications of thermistor composition are proprietary information, general information is that NTC thermistors are made of Mn_3O_4 and PTC thermistors are of Sr-doped $BaTiO_3$. Properties of these materials are given in Table 6 with physical dimensions for the thermistor mountings. The calculated and measured time constants (by Method 2) for $t_{NTC,1}$ as a function of N_s with $r_s = 1.63$ cm are plotted in Fig. 5.

The dissipation constant, δ_t, measured for an NTC thermistor as a function of N_s showed no variation for $400 < N_s < 2000$ rev min^{-1} with $r_s = 1.27$ cm. Calculated and measured values of δ_t for a PTC thermistor are plotted in Fig. 6 as a function of N_s. Agreement between experimental and predicted values is good

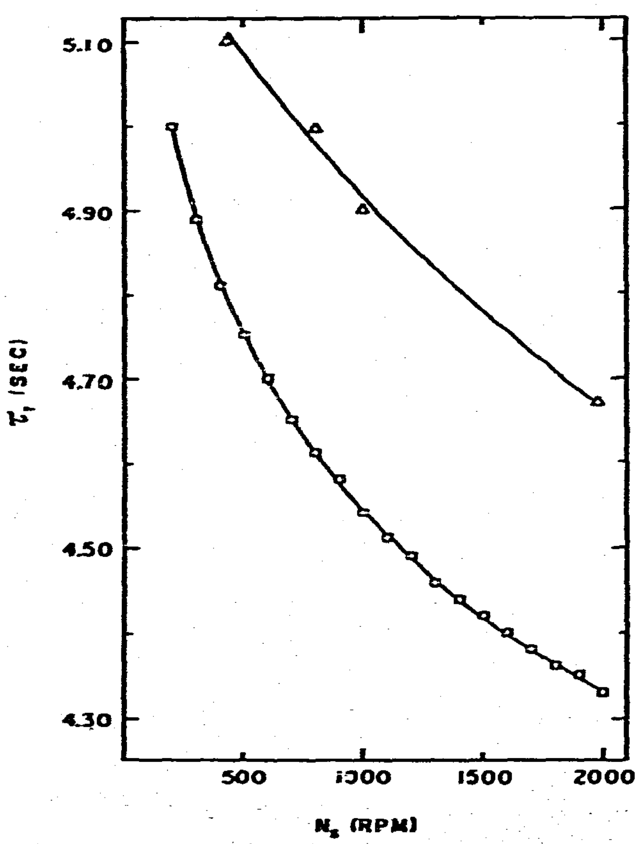

Fig. 5. Time constant of thermistor t_1 as a function of N_s. □, calculated; △, experimental.

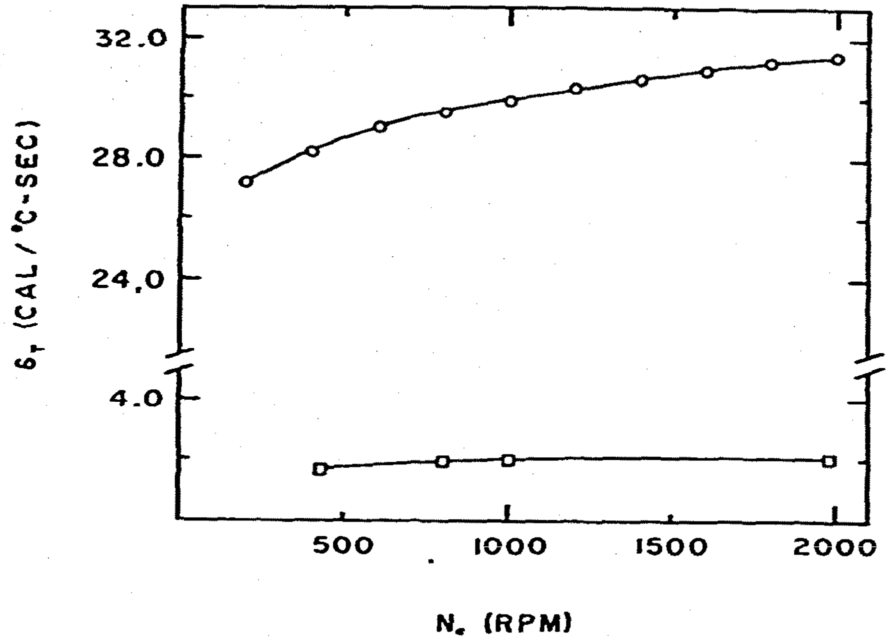

Fig. 6. NTC and PTC thermistor dissipation constants as a function of N_s. O, calculated; □, experimental.

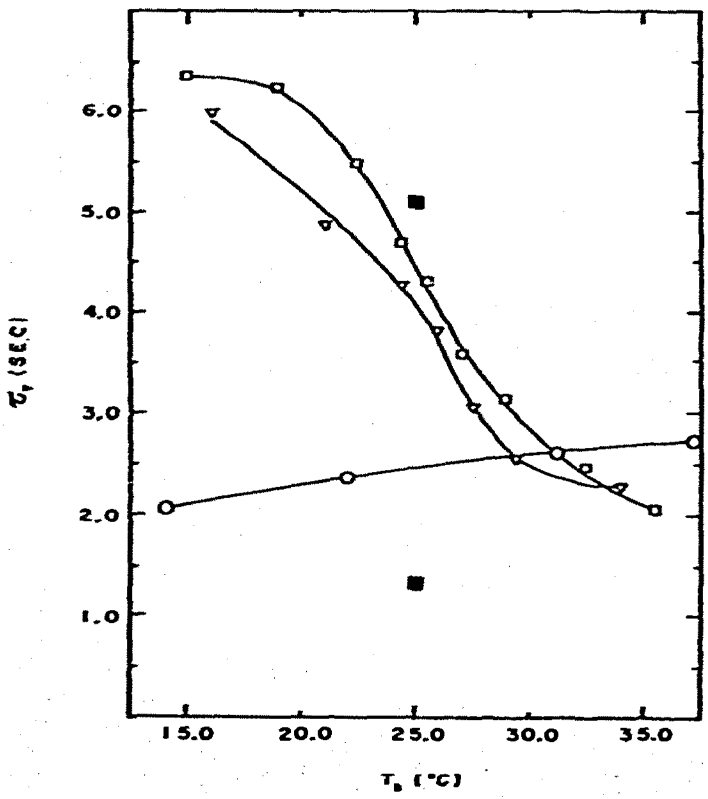

Fig. 7. NTC and PTC thermistor time constants as a function of T. O, NTC; □, PTC; ▽, NTC–PTC; ■ (upper), PTC calculated, and ■ (lower), NTC calculated.

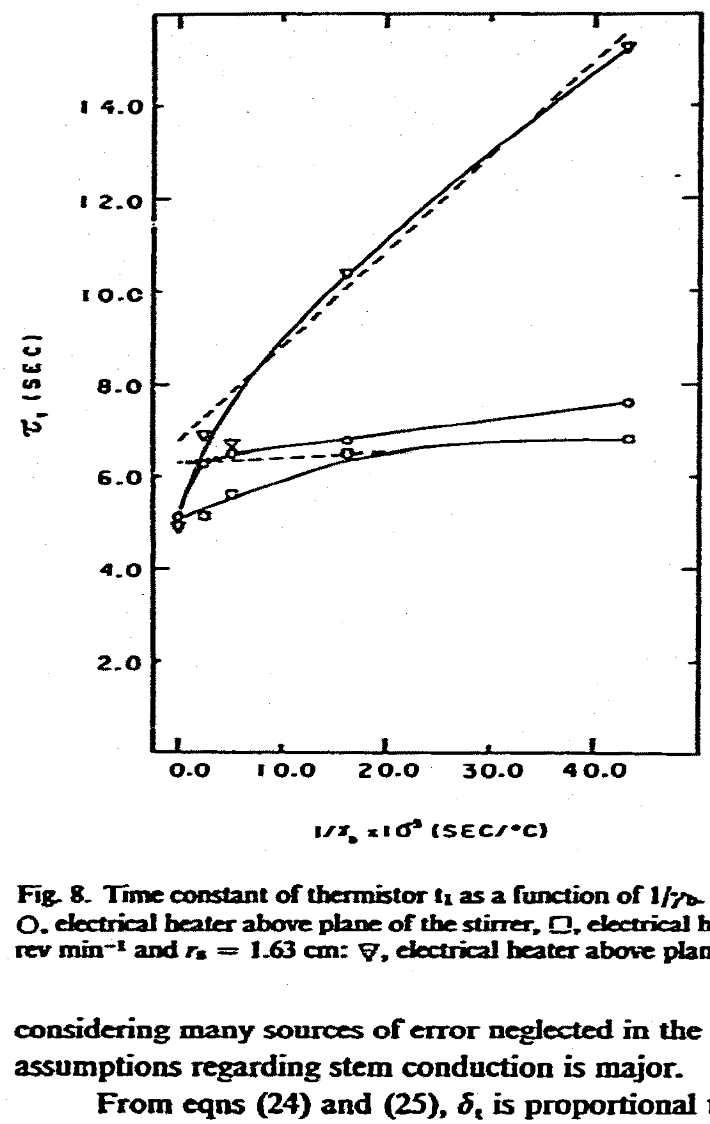

Fig. 8. Time constant of thermistor t_t as a function of $1/\gamma_b$. N_s = 430 rev min^{-1} and r_s = 1.63 cm: O, electrical heater above plane of the stirrer, □, electrical heater in plane of the stirrer; N_s = 1000 rev min^{-1} and r_s = 1.63 cm: ▽, electrical heater above plane of the stirrer.

considering many sources of error neglected in the theoretical development of which assumptions regarding stem conduction is major.

From eqns (24) and (25), δ_t is proportional to r_t and τ_t is proportional to r_t^2. This has been demonstrated for bead thermistors[45]. It is beyond question that an epoxy coating on the thermistor will change both δ_t and τ_t. The usual coating material is glass which has a thermal conductivity about 4 × that of most plastics. The effects of various thermistor coatings was experimentally shown by Rogers and Sasiela[46]. Experimentally measured values of τ_t for a NTC and PTC thermistor are given in Fig. 7 as a function of temperature. It is interesting that the plots are mirror images of dR_t/dT_t for both thermistors as predicted by eqn (36).

Careful examinations of eqns (18) and (19) reveals that the temperature difference across the thermistor material and across the epoxy plus thermal boundary layers can be calculated. Such calculations show that the predominant difference is across the epoxy plus thermal boundary layer; the ratio of the differences is 35:1.

The dependence of τ_t upon γ_b as predicted by eqn (32) was studied by heating the calorimeter bulk solution at four rates. The experimental results are given in Fig. 8.

The values of curve intercepts were those obtained in a study of τ_t vs. N_s for a step change in the temperature of the fluid surrounding the thermistor. Differences in the intercepts in Fig. 8 as determined by Method 2 in comparison to those from electrical heating experiments is due to the time of fluid mixing and the time constant of the electrical heater. Although not shown in Fig. 8, the predicted decrease in the slope of τ_t vs. $1/\gamma_b$ plot with increase of P_t was verified experimentally. Placement of the electrical heater affects the relationship of τ_t to $1/\gamma_b$ since incomplete mixing leads to underdamping of the system response. Larger values of N_s lead to overdamping which produces increased slope as seen in Fig. 8 for $N_s = 1000$ rev min^{-1}. More will be said concerning heater placement in a later publication.

APPENDIX

List of symbols

a, a_1, a_2, b, c, d, m, n coefficients

α_n	roots of the transcendental equation $r_t\alpha_n \cot r_t\alpha_n + r_t h - 1 = 0$
α_t	Material coefficient of thermistor with positive temperature coefficient (1/°K)
A_e	cross section area of epoxy filling plus Teflon tubing in thermistor mounting (cm^2)
A_t	total cross sectional area of thermistor stem (cm^2)
A_w	cross sectional area of thermistor lead wires (cm^2)
β_t	material coefficient of thermistor with negative temperature coefficient (K)
c_b	mass heat capacity of bulk solution (cal g^{-1} °C^{-1})
c_t	volume heat capacity of thermistor material (cal cm^{-3} °C^{-1})
c_t'	mass heat capacity of thermistor material (cal g^{-1} °C^{-1})
C_t	heat capacity of thermistor (cal °C^{-1})
C_f	feedback capacitor for operational amplifier 3 in Fig. 1 (μF)
D_b	thermal diffusivity of bulk solution (cm^2 sec^{-1})
D_t	thermal diffusivity of thermistor material (cm^2 sec^{-1})
δ_b	dissipation constant of epoxy plus stem and boundary layer (cal sec^{-1} °C^{-1})
δ_0	dissipation constant of thermistor bead (cal sec^{-1} °C^{-1})
δ_t	dissipation constant of thermistor assembly (cal sec^{-1} °C^{-1})
e_+, e_-	positive and negative voltages applied to thermistors t_2 and t_1, respectively (V)
$e_{o,3}$	output voltage of Operational Amplifier 3 in Fig. 1 (V)
γ_b	heating rate of bulk solution (°C sec^{-1})
γ_t	heating rate of thermistor by electrical power (°C sec^{-1})
h	h_t/λ_{eq} (1/cm)
h_s	convective heat transfer coefficient of thermistor stem (cal cm^{-2} sec^{-1} °C^{-1})
h_t	convective heat transfer coefficient of thermistor bead (cal cm^{-2} sec^{-1} °C^{-1})
λ_b	thermal conductivity of bulk solution (cal cm^{-1} sec^{-1} °C^{-1})
λ_e	thermal conductivity of epoxy (cal cm^{-1} sec^{-1} °C^{-1})
λ_{eq}	equivalent thermal conductivity of thermistor material plus epoxy and stem (cal cm^{-1} sec^{-1} °C^{-1})

λ_i	inner thermal conductivity of thermistor material corrected for epoxy and stem effects (cal cm^{-1} sec^{-1} $°C^{-1}$)
λ_s	equivalent thermal conductivity of thermistor stem (cal cm^{-1} sec^{-1} $°C^{-1}$)
λ_t	thermal conductivity of thermistor material (cal cm^{-1} sec^{-1} $°C^{-1}$)
λ_w	thermal conductivity of thermistor lead wires (cal cm^{-1} sec^{-1} $°C^{-1}$)
N_s	rotation speed of stirrer (rev min^{-1})
ν_b	kinematic viscosity of bulk solution (cm^2 sec^{-1})
ω_s	angular velocity of stirrer (rad sec^{-1})
P_t	electrical power applied to thermistor (cal sec^{-1})
r_c	radius of calorimeter cell (cm)
r_s	radius of stirrer disk (cm)
r_{st}	radius of thermistor stem (cm)
r_t	radius of thermistor bead (cm)
ρ_t	mass density of thermistor material (g cm^{-3})
R_f	feedback resistance of operational amplifier 3 in Fig. 1 (Ω)
R_t	resistance of thermistor at its geometric center (Ω)
t	time (sec)
t	thermistor
T_b	bulk solution temperature (K)
T_t	thermistor temperature at the geometric center (K)
τ_b	time constant of epoxy plus stem and boundary layer (sec)
τ_0	time constant of thermistor bead (sec)
τ_t	time constant of thermistor assembly (sec)
U	fluid velocity
x_e	thickness of epoxy film on thermistor (cm)
x_s	length of thermistor stem (cm)
Z_t	pre-exponential term in thermistor resistance functions (Ω)

REFERENCES

1 F. T. Wooten, *Proc. IEEE*, 55 (1967) 564.
2 H. W. Linde, L. B. Rogers and D. N. Hume, *Anal. Chem.*, 25 (1953) 404.
3 B. C. Tyson, W. H. McCurdy and C. E. Bricker, *Anal. Chem.*, 33 (1961) 1640.
4 S. N. Hajiev and M. J. Agarunov, *Temperature, Its Measurement and Control in Science and Industry*, Vol. 4, part 2, Reinhold, New York, 1972, pp. 1065–1069.
5 S. Johansson, *Ark. Kemi*, 24 (1964) 189.
6 H. J. V. Tyrrell and A. E. Beezer, *Thermometric Titrimetry*, Chapman and Hall, London, 1968, pp. 46–68.
7 L. S. Bark and S. M. Bark, *Thermometric Titrimetry*, Pergamon Press, London, 1969, pp. 21–41.
8 R. C. LaForce, S. F. Ravitz and W. B. Kendall, *Rev. Sci. Inst.*, 35 (1964) 729.
9 E. B. Smith, C. S. Barnes and P. W. Parr, *Anal. Chem.*, 44 (1972) 1663.
10 S. H. Ediz, M. van Swaay and H. D. McBride, *Chem. Instrum.*, 3 (1972) 299.
11 C. E. Vanderzee and J. A. Swanson, *J. Phys. Chem.*, 67 (1963) 285.
12 K. J. Jahr, G. Weise and G. Schluchardt, *Z. Phys. Chem.*, 61 (1968) 73.
13 H. W. Trolander, D. A. Case and R. W. Harruf, *Temperature, Its Measurement and Control in Science and Industry*, Vol. 4, part 2, Reinhold, New York, 1972, p. 1002.
14 M. J. Bowman and F. H. Sagar, *IEEE Trans.*, IM-21 (1972) 48.

15 D. Buhl, *Anal. Chem.*, 40 (1968) 715.
16 N. E. Vanderborgh and W. D. Spall, *Anal. Chem.*, 40 (1968) 256.
17 R. W. A. Scarr and R. A. Setterington, *Proc. IEEE*, 107B (1960) 395.
18 M. Prudenziati, A. Taroni and G. Zanarini, *IEEE Trans., IECI-17* (1971) 407.
19 E. Andrich, *Philips Tech. Rev.*, 30 (1969) 170.
20 H. A. Sauer and J. R. Fisher, *J. Am. Ceram. Soc.*, 43 (1960) 297.
21 G. N. Tekster-Proskuryakova and I. T. Sheftel, *Radio Eng. Electron. Phys.*, 5 (1966) 781.
22 H. S. Carslaw and J. C. Jaeger, *Conduction of Heat in Solids*, Clarendon Press, London, 1959, pp. 237–246.
23 R. A. Rasmussen, *Rev. Sci. Inst.*, 33 (1962) 38.
24 Y. V. Kudryavtsev, et al., *Unsteady-State Heat Transfer*, Iliffe Books, London, 1966, p. 86.
25 S. S. Kutateladze, *Fundamentals of Heat Transfer*, Academic Press, New York, 1963, pp. 242–244.
26 J. W. Murdock, C. J. Foltz and C. Gregory, *Trans. ASME, J. Eng. Power*, 85 (1963) 27.
27 A. W. Rice, H. L. Toor and F. S. Manning, *A. I. Ch. E. J.*, 10 (1964) 125.
28 C. Papadopoulos, *Chem. Ind. (London)*, 33 (1971) 932.
29 R. S. Brodkey, *A. I. Ch. E. J.*, 9 (1963) 448.
30 M. Dutt and T. Stickney, *ISA Trans.*, 9 (1970) 81.
31 R. P. Benedict, *Fundamentals of Temperature, Pressure, and Flow Measurements*, Wiley, New York, 1969, p. 162.
32 M. D. Scadron and I. Warshawsky, *Experimental Determination of Time Constants and Nusselt Numbers for Bare-Wire Thermocouples in High Velocity Air Streams and Analytic Approximation of Conduction and Radiation Errors*, NACA, TN 2599, Jan., 1952.
33 P. G. Stecher (Ed.), *The Merck Index*, Merck, Rathway, N. J., 8th ed., 1968, p. 810.
34 J. F. Swindells, *Calibration of Liquid in Glass Thermometers*, National Bureau of Standards Monograph 90, National Bureau of Standards, Washington, D.C., 1965, pp. 12–13.
35 L. C. Pharo, *Rev. Sci. Inst.*, 36 (1965) 211.
36 A. E. Van Til, *Ph. D. Dissertation*, Iowa State University, Ames, Iowa 1976.
37 D. P. Wrathall and W. L. Gardner, *Temperature, Its Measurement and Control in Science and Industry*, Vol. 4, part 3, Reinhold, New York, 1972, p. 2223.
38 L. D. Hansen and E. A. Lewis, *Anal. Chem.*, 43 (1971) 1393.
39 OM. N. Bhatnagar and A. N. Campbell, *Chem. Instrum.*, 4 (1973) 179.
40 I. M. Gottlieb, *Regulated Power Supplies*, H. W. Sams and Co., Indianapolis, Ind., 1971, p. 70.
41 R. C. Weast (Ed.), *Handbook of Chemistry and Physics*, 47th edition, Chemical Rubber Co., Cleveland, Ohio, 1967.
42 Y. S. Touloukian, R. W. Powell, C. Y. Ho and P. G. Klemens, *Thermophysical Properties of Matter, Thermal Conductivity, Nonmetallic Solids*, Vol. 2, Plenum Press, New York, 1970, p. 257.
43 Y. S. Touloukian and E. H. Buyco, *Thermophysical Properties of Matter, Specific Heat, Nonmetallic Solids*, Vol. 5, Plenum Press, New York, 1970, p. 1313.
44 H. Lee and K. Neville, *Handbook of Epoxy Resins*, McGraw Hill, New York, 1967, pp. 6–32.
45 *Catalog MGP 681*, Victory Engineering Corp., Springfield, N.J., 1967, p. 5.
46 D. W. Rogers and R. J. Sasiela, *Talanta*, 20 (1972) 232.